Quench Protection of a Nb_3Sn Superconducting Magnet System for a 45 GHz ECR Ion Source

E. Ravaioli, A. Hafalia, M. Juchno, W. Lu, GL. Sabbi, L. Sun, W. Wu, D. Xie, H.W. Zhao, and S.J. Zheng

***Abstract*—Lawrence Berkeley National Laboratory (LBNL) in collaboration with the Institute of Modern Physics (IMP) has developed a Nb_3Sn-based superconducting magnet system for a fourth-generation Electron Cyclotron Resonance (ECR) source, with a goal of achieving the magnetic field required for operating at the microwave frequency of 45 GHz. The magnet system is composed of one sextupole magnet inside three solenoids of different sizes manufactured from Nb_3Sn round wire. Given the high stored energy density and relatively low wire copper fraction, the coils are not self-protected in the case of a quench. The study of the transient following a quench is carried out by means of the LEDET (Lumped-Element Dynamic Electro-Thermal) program, which includes a detailed simulation of the inter-filament coupling losses developing in the wire. Non-linear effects occurring in the magnet, such as coupling loss and differential inductance reduction, have a significant impact on protecting these magnets. The resulting baseline quench protection strategy based on four independent energy extraction systems protecting the four magnets meets the quench protection requirements. Furthermore, in order to enhance the redundancy of the quench protection system and reduce the peak voltages to ground, the implementation of a CLIQ (Coupling-Loss Induced Quench) system is considered.**

***Index Terms*—circuit modeling, CLIQ, ECR, quench protection, superconducting coil.**

I. Introduction

THE Nb_3Sn-based superconducting magnet system for a fourth-generation 45 GHz Electron Cyclotron Resonance (ECR) source has been designed by the Lawrence Berkeley National Laboratory (LBNL) in collaboration with the Institute of Modern Physics (IMP) [1].

The sextupole-in-solenoid system, represented in Fig. 1, includes a 857 mm long sextupole magnet (S), a 30 mm long middle solenoid (M), a 60 mm long extraction solenoid (E), and two 60 mm long injection solenoids (I). All magnets are fabricated with the same Nb_3Sn round wire and supported by a single mechanical structure [1], [2]. The larger injection solenoid is split into two modules due to mechanical considerations [2], wire piece length availability, and quench protection.

The magnet and conductor design parameters, summarized in Tables I and II [1], make the protection of these magnets after a quench considerably more challenging than in conventional Nb-Ti based ECR source magnets [3]. First, the higher energy density stored in the conductor due to the higher magnetic field increases the potential for damage. Second, the normal-zone propagation velocities in the low-field regions are reduced due to higher thermal margin to quench. Third, the stabilizer fraction in Nb_3Sn internal tin wire is limited to lower range than Nb-Ti wire, which increases the stabilizer current density. Fourth, the choice of wire instead of cable as a conductor, to avoid the cabling process and to limit the operating current, significantly increases the magnets' self-inductances and decreases the turn-to-turn normal-zone

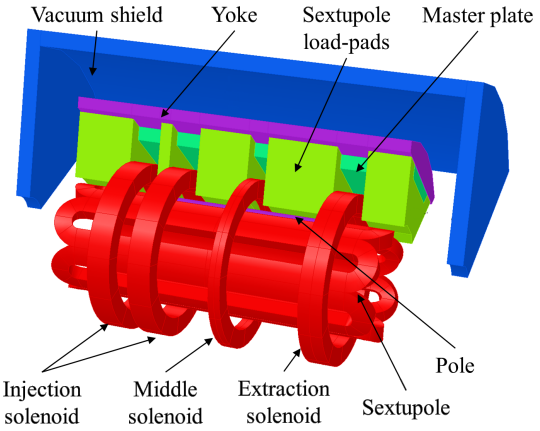

Fig. 1. Simplified 3D representation of the 45 GHz ion source magnet system.

TABLE I
Main Parameters of the Four Magnets [1].

Parameter	Unit	S	M	E	I
Nominal current, I_{nom}	A	654	380	626	692
Peak conductor field at I_{nom}	T	11.3	5.0	9.7	11.8
Operating temperature	K	4.2	4.2	4.2	4.2
Inner diameter	mm	200	336	336	336
Outer diameter	mm	276	430	430	430
Magnet length	mm	862	30	60	2x60
Conductor packing factor	-	0.65	0.70	0.70	0.70

TABLE II
Main Conductor Parameters [1].

Parameter	Unit	Value
Critical current density at 4.2 K, 12 T	kAmm^{-2}	2.4
Wire diameter	mm	1.3
Copper/non-Copper ratio	-	0.96
RRR of the copper matrix	-	250
Filament twist pitch	mm	42
Insulation thickness	μm	65

Work supported by the US Department of Energy through the US LHC Accelerator Research Program (LARP) and NSFC (Contract No. 11427904).

E. Ravaioli, A. Hafalia, M. Juchno, W. Lu, GL. Sabbi, and D. Xie are with the Lawrence Berkeley National Laboratory, Berkeley, CA. (e-mail: ERavaioli@lbl.gov).

L. Sun, W. Wu, H.W. Zhao, and S.J. Zheng are with the Institute of Modern Physics, Chinese Academy of Sciences, Lanzhou, China.

Manuscript received August 29, 2017.

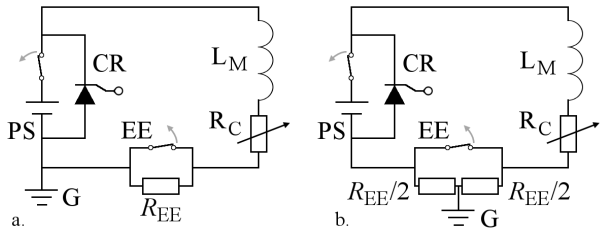

Fig. 2. Simplified electrical schematic of one of the four magnet circuits, including a power supply (PS), its crowbar (CR), the magnet (L_M), its resistance developing during a quench (R_C), an energy-extraction system (EE), and the grounding (G). a. Standard grounding. b. Symmetric grounding.

propagation speed.

The protection of each magnet is analyzed separately maintaining common requirements in terms of maximum allowed hot-spot temperature $T_{\rm hot}$ [K] and voltage to ground $U_{\rm g}$ [V]. The maximum values of $T_{\rm hot}$ and $U_{\rm g}$ are set to 350 K [4] and 1 kV, respectively.

The baseline quench protection systems for the four magnets, based on energy-extraction (EE), are presented. The alternative protection system based on CLIQ [5]–[7] is investigated for the sextupole magnet protection. The analysis is performed with the LEDET (Lumped-Element Dynamic Electro-Thermal) program [5], [8], [9], which includes non-linear effects such as inter-filament coupling loss, quench-back, and reduction of the differential inductance due to coupling currents.

II. Energy-Extraction Quench Protection

It can be easily shown that self-protection is not a viable option for any of the four magnets [1]. Even in the case of the shortest M solenoid, $T_{\rm hot}$ reaches around 400 K, which is higher than the 350 K limit. Therefore, an active system is required, which detects the quench, switches off the power supply, and quickly discharges the magnet transport current $I_{\rm m}$ [A]. The baseline powering and quench protection strategy features an independent power supply and energy-extraction system for each of the four magnets. The simplified electrical schematic of one of the four circuits is shown in Fig. 2a. Upon quench detection, the energy-extraction switch is opened and the current is discharged due to the energy-extraction resistance $R_{\rm EE}$ [Ω] and coil resistance $R_{\rm C}$ [Ω]. $R_{\rm EE}$ is selected for each magnet as a compromise between a quick current discharge, calling for high resistance, and a low voltage to ground, calling for low resistance.

The peak voltage across the EE resistor, reached just after EE triggering, is $U_{\rm EE}$=$R_{\rm EE}I_0$, with I_0 [A] the initial magnet current. This is the peak voltage to ground reached in the circuit during the quench transient, $U_{\rm g}$=$U_{\rm EE}$. However, it is possible to halve $U_{\rm g}$ by symmetrically grounding the circuit at the middle point of the EE resistor, as shown in Fig. 2b, hence obtaining $U_{\rm g}$≈$U_{\rm EE}/2$.

Based on the experience with similar superconductors working at similar magnetic fields and current densities, it is assumed that quench detection and validation is performed in 15 ms. The energy-extraction switching mechanism includes a silicon controlled rectifier (SCR), opening in 2 ms, and a mechanical switch, opening in 32 ms, connected in series for redundancy. Thus, the EE triggering time is 2 ms in absence of failures and 32 ms in the case of SCR failure.

The protection of each magnet is analyzed separately, neglecting the magnetic coupling between them. This approach is conservative considering that the mutual inductances between magnets are either negative or much lower than their self-inductances, as shown in Table III.

TABLE III
Magnet Self- and Mutual Inductances in Units of H.

	S	M	E	I
S	2.40	0.00	0.00	0.00
M	0.00	0.35	-0.08	-0.16
E	0.00	-0.08	1.27	0.08
I	0.00	-0.16	0.08	3.46

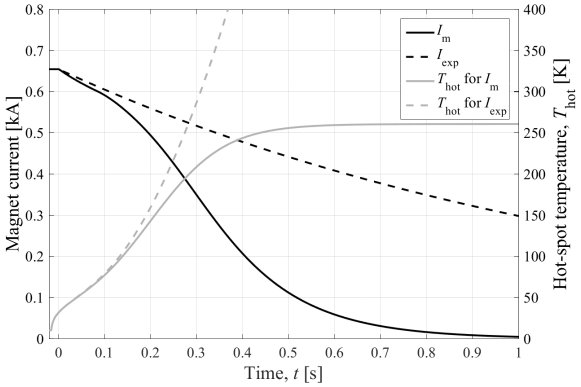

Fig. 3. Energy-extraction discharge of the sextupole magnet. Simulated current $I_{\rm m}$ and hot-spot temperature $T_{\rm hot}$ versus time after a quench at nominal current protected by a 2 Ω energy-extraction system. The current $I_{\rm exp}$ calculated for a purely exponential decay and the resulting $T_{\rm hot}$ are also provided.

A. Effect of Coupling Currents on Energy-Extraction Discharge

In the absence of non-linear effects, after triggering the energy-extraction system the magnet current decay is purely exponential and follows $I_{\rm m}(t)$=$I_{\rm exp}(t)$=$I_0\exp(-tR_{\rm EE}/L_{\rm M})$, with $L_{\rm M}$ [H] as the magnet self-inductance. However, the presence of inter-filament coupling currents significantly influences the electro-magnetic and thermal transient [9]. First, the magnet differential inductance is reduced due to the coupling currents generated in the wires. Second, the heat deposited as inter-filament coupling loss increases the local wire temperature and can cause a transition to the normal state of significant parts of the coil, hence increasing the coil resistance.

As an example, the simulated current after a quench in the sextupole magnet's highest-field turn at the nominal operating current $I_{\rm nom}$=654 A (t=−15 ms) and subsequent triggering of a 2 Ω EE system (t=2 ms) is shown in Fig. 3. The magnet current decays significantly more quickly than a purely exponential decay. In the presented case, $I_{\rm m}$ and $I_{\rm exp}$ differ by 10% at t=193 ms, and by 50% at t=380 ms. This change

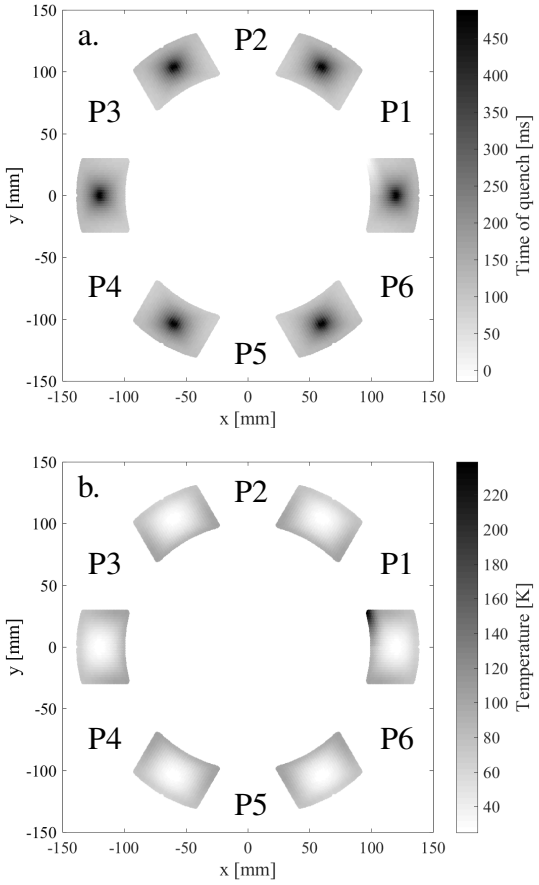

Fig. 4. Energy-extraction discharge of the sextupole magnet (I_0=654 A, $R_{\rm EE}$=2 Ω). Quench starts at t=−15 ms in the highest-field wire of pole P1 and EE is triggered at t=2 ms. a. Simulated time at which each wire is transferred to the normal state. b. Simulated temperature profile in the cross-section of the magnet at the end of the discharge.

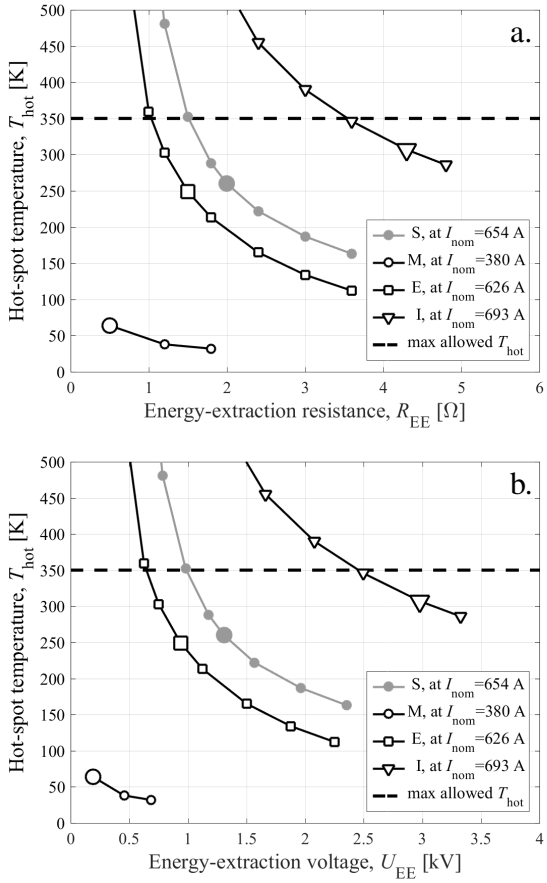

Fig. 5. Energy-extraction discharge of the four magnets. Simulated hot-spot temperature after a quench at nominal current. a. As a function of the energy-extraction resistance. b. As a function of the peak voltage across the energy-extraction resistor. Larger markers indicate design values shown in Table IV.

occurs when large parts of the coil are transferred to the normal state due to inter-filament coupling loss, which reaches a peak power deposition of a few mWmm^{-3}. The time at which each wire is transferred to the normal state is plotted in Fig. 4a. About 19%, 62% and 80% of the wire volume is quenched 100, 150, and 200 ms after EE triggering, respectively.

The simulated temperature profile at the end of the discharge is shown in Fig. 4b. The temperature remains between 25 to 100 K in the bulk of the magnet, but it reaches about 240 K in the turn where the quench started. The hot-spot temperature calculated under the more conservative assumption of adiabatic condition, plotted in Fig. 3, reaches about 260 K, well below the maximum allowed temperature of 350 K. In the case of the simple exponential decay, $T_{\rm hot}$ reaches well above 400 K, as shown in Fig. 3. This result indicates that quench-back is determinant for this magnet's quench protection with energy extraction.

B. Energy-Extraction System Optimization

Similar discharges are simulated for each magnet circuit at its respective $I_{\rm nom}$ for varying EE resistances. The calculated hot-spot temperatures are plotted in Fig. 5a and Fig. 5b as a function of $R_{\rm EE}$ and $U_{\rm EE}$, respectively. For each circuit, the optimum value of $R_{\rm EE}$, which maintains $T_{\rm hot}$ below 350 K with sufficient margin while minimizing $U_{\rm g}$, is determined. The $R_{\rm EE}$ values selected for the four circuits and the resulting $U_{\rm g}$ and $T_{\rm hot}$, in nominal and SCR failure cases, are tabulated in Table IV.

TABLE IV
SUMMARY OF THE ENERGY-EXTRACTION SYSTEM PERFORMANCE.

Parameter	Unit	S	M	E	I
EE resistor $R_{\rm EE}$	Ω	2.0	0.5	1.5	4.3
Peak voltage to ground, $U_{\rm g}$	V	654	95	470	1488
Hot-spot temperature, $T_{\rm hot}$	K	260	64	249	315
$T_{\rm hot}$ in case of SCR failure	K	337	70	318	410

Note: In absence of symmetric grounding, all values of $U_{\rm g}$ double.

The protection of the M and E solenoids can be achieved with $R_{\rm EE}$ values of 0.5 and 1.5 Ω, respectively. With this choice, even in the case of SCR failure $T_{\rm hot}$ is maintained safely below the 350 K temperature limit. Besides, $U_{\rm g}$ remains below 1 kV even in the case of non-symmetric grounding.

The protection of the two I solenoids in series can be attained with a 4.3 Ω EE system. However, the target of 1 kV limit on $U_{\rm g}$ is overcome by a factor 1.5 and 3 in the case of symmetric or non-symmetric grounding, respectively.

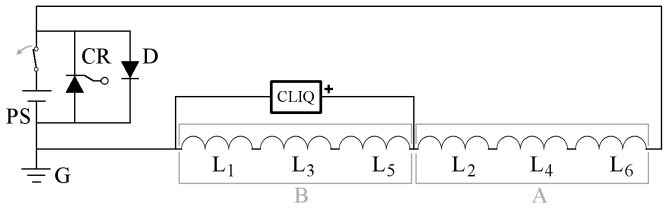

Fig. 6. Simplified electrical schematic of the sextupole circuit with CLIQ-based quench protection. L_1-L_6 are the six poles, numbered counter-clockwise, as shown in Fig. 4.

Furthermore, in the case of SCR failure, the 350 K limit on $T_{\rm hot}$ is exceeded.

A possible solution to mitigate these problems is powering the two I solenoids in separate circuits. This option results in halving the peak voltage to ground, but at the cost of doubling the power supplies, energy-extraction systems, and current leads required for the I solenoids. In addition, the redundancy of the EE system could be improved, for example including several SCRs in series instead than one SCR in series to a slower mechanical switch.

The quench protection of the sextupole magnet can be achieved with a 2 Ω EE system. However, in the case of SCR failure $T_{\rm hot}$=337 K, close to the maximum allowed temperature. Given the uncertainties in the model assumptions, wire parameters, and material properties, this margin is unsatisfactory. Furthermore, if symmetric grounding cannot be implemented, the 1 kV limit on $U_{\rm g}$ is also exceeded. Therefore, protection of the sextupole magnet with energy-extraction is marginal.

III. Sextupole Magnet CLIQ-Based Protection

Powering and protecting separately sections of the sextupole magnet is a viable option. However, this solution is not preferred since introducing even a minor imbalance in the currents flowing through the different poles would reduce the system operation performance. Thus, an alternative approach to quench protection, based on CLIQ, is under consideration, which can improve the system redundancy and reduce the peak voltages to ground without the need of doubling the powering and energy-extraction circuits. CLIQ relies on a capacitive discharge method that introduces fast current changes in the coil sections [5]–[7]. The resulting fast changes of the local magnetic field introduce high inter-filament coupling loss [10], [11], which in turn causes the heating of the conductor and a transition to the normal state of voluminous coil parts. This technology was successfully applied for the protection of multi-pole magnets [7], [12]–[14] and solenoids [15].

In order to maximize the effectiveness of a CLIQ system, opposite current changes should be introduced into physically adjacent coil sections [16]. Applying this criterion to the sextupole geometry, an optimized system is obtained by selecting the pole electrical order and CLIQ terminal positioning shown in Fig. 6. This configuration only requires one CLIQ terminal connected to the coil's middle point.

As an example, the transient following a quench at nominal current in the S magnet and the subsequent protection using a

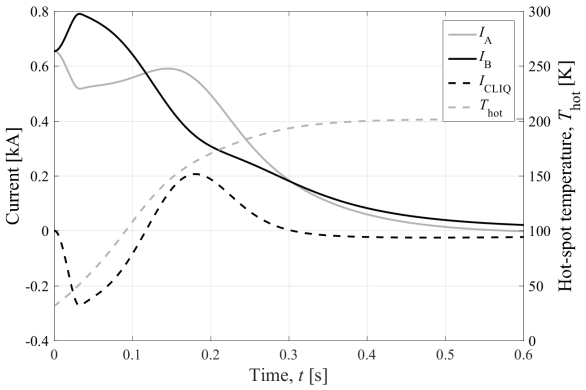

Fig. 7. Discharge of the sextupole magnet with a 200 V, 80 mF CLIQ unit. Simulated currents in the coil sections $I_{\rm A}$ and $I_{\rm B}$, current introduced by CLIQ $I_{\rm C}$, and hot-spot temperature $T_{\rm hot}$ after a quench at nominal current, versus time.

200 V, 80 mF CLIQ unit is presented in Fig. 7. The current $I_{\rm C}$ [A] introduced by CLIQ is roughly equally distributed between the two coil sections A and B, each composed of three poles (see Fig. 6). As a result, the currents in the coil sections $I_{\rm A}$ and $I_{\rm B}$ [A] oscillate, as shown in Fig. 7. The coupling loss due to the consequent magnetic-field change in the wires reaches a peak of about 28 mWmm^{-3}. The fast transition to the normal state induced by this local heating causes the coil resistance to rise rapidly, hence quickly discharging the magnet current. The calculated adiabatic hot-spot temperature, also plotted in Fig. 7, is 202 K, lower than that obtained using the baseline 2 Ω EE system.

The speed of the transition to the normal state can be observed in Fig. 8a. About 52% and 95% of the coil volume is quenched 50 ms and 100 ms after triggering CLIQ, respectively. As a result, the temperature distribution in the magnet cross-section is rather homogeneous, as shown in Fig. 8b. The temperature reaches 45 to 135 K in the bulk of the magnet, and 190 K in the turn where the quench started.

Similar discharges for varying values of capacitance and charging voltage of the CLIQ unit are simulated. The calculated hot-spot temperatures are plotted in Fig. 9 as a function of the peak voltage to ground during the transient. With a 40 or 80 mF CLIQ unit charged to voltages in the range 200 to 300 V it is possible to maintain $T_{\rm hot}$ around 200 K and $U_{\rm g}$ below 500 V. The transient shown in Fig. 7 is obtained with optimum 200 V, 80 mF CLIQ parameters, which achieve $U_{\rm g}$=360 V. In comparison, to maintain $T_{\rm hot}\leq$200 K using an EE system $U_{\rm g}$ reaches values 2.5 or 5 times higher with standard or symmetric grounding, respectively, as can be observed in Fig. 9.

IV. Conclusion

The quench protection of a sextupole-in-solenoid Nb_3Sn magnet system for a 45 GHz ECR ion source is analyzed. The baseline design consists of four independent circuits, each protected by an energy-extraction system whose resistor is optimized for each specific magnet.

Non-linear effects, such as inter-filament coupling loss and differential-inductance reduction due to coupling currents,

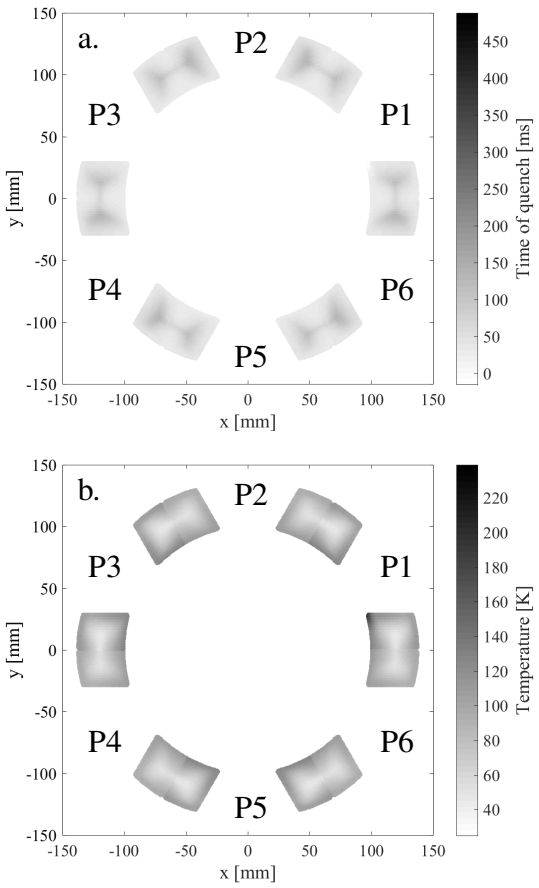

Fig. 8. Discharge of the sextupole magnet with a 200 V, 80 mF CLIQ unit (I_0=654 A). Quench starts at t=−15 ms in the highest-field wire of pole P1 and EE is triggered at t=2 ms. a. Simulated time at which each wire is transferred to the normal state. b. Simulated temperature profile in the cross-section of the magnet at the end of the discharge. The scales used in these plots are the same used in Fig. 4.

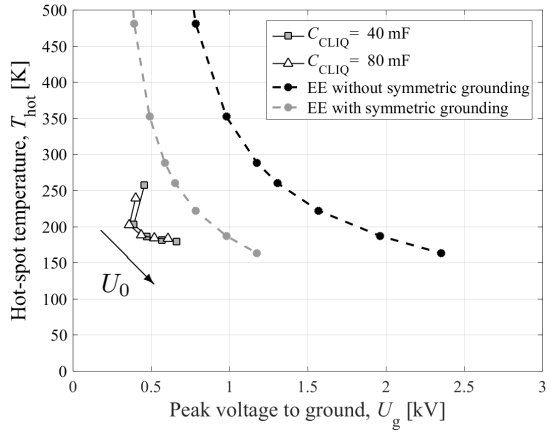

Fig. 9. Simulated hot-spot temperature after a quench at nominal current in the sextupole magnet as a function of the peak voltage to ground, for CLIQ units of capacitance 40 and 80 mF and charging voltage U_0 in the range 150 to 500 V. Comparison with $T_{\rm hot}$ and $U_{\rm g}$ obtained by using an EE system.

have a determinant impact on these magnets' quench protection performances. Thus, the analysis was carried out with the LEDET program, which simulates these effects with an equivalent lumped-element network approach.

The baseline energy-extraction system achieves a performance compatible with the target limits of 350 K on the hot-spot temperature and 1 kV on the peak voltage to ground only for the protection of the middle and extraction solenoids. On the contrary, in the case of the sextupole magnet and two injection solenoids, the hot-spot temperature reaches values close or above 350 K in a failure case causing a delay of 30 ms of the energy-extraction opening. Furthermore, the sextupole's peak voltage to ground can be maintained below 1 kV only by implementing symmetric grounding of the circuit, and the injection solenoids' only by implementing symmetric grounding and powering separately the two solenoids.

For these reasons, an alternative CLIQ-based protection system was investigated. With this active heating system, a large fraction of the coil is rapidly transferred to the normal state and the magnet's stored energy is distributed rather homogeneously within the turns. In the case of the sextupole magnet, a resulting hot-spot temperature well below the target limit can be achieved while developing significantly lower peak voltages to ground than an energy-extraction system. A similar system for the protection of the injection solenoids can be analyzed in the future.

REFERENCES

[1] G. Sabbi, A. Hafalia, M. Juchno, W. Lu, E. Ravaioli, L. Sun, and D. Xie, "Design of the Superconducting Magnet System for a 45 GHz ECR Ion Source," Tech. Rep., 2017.

[2] M. Juchno, A. Hafalia, W. Lu, E. Ravaioli, G. Sabbi, L. Sun, W. Wu, D. Xie, H. Zhao, and L. Zhu, "Mechanical design of a Nb_3Sn superconducting magnet system for a 45 GHz ECR ion source," *IEEE Transactions on Applied Superconductivity*, to be published.

[3] C. Taylor, S. Caspi, M. Leitner, S. Lundgren, C. Lyneis, D. Wutte, S. T. Wang, and J. Y. Chen, "Magnet system for an ecr ion source," *IEEE Transactions on Applied Superconductivity*, vol. 10, no. 1, pp. 224–227, March 2000.

[4] G. Ambrosio, "Maximum allowable temperature during quench in Nb_3Sn accelerator magnets," in *Proceedings, WAMSDO 2013 Workshop on Accelerator Magnet, Superconductor, Design and Optimization: CERN Geneva, Switzerland, 15-16 Jan 2013*, 2013, pp. 43–46. [Online]. Available: https://inspirehep.net/record/1277941/files/arXiv:1401.3955.pdf

[5] E. Ravaioli, "CLIQ," Ph.D. dissertation, Enschede, 2015, presented on 19 June 2015. [Online]. Available: http://doc.utwente.nl/96069/

[6] V. Datskov, G. Kirby, and E. Ravaioli, "AC-current induced quench protection system," Patent EP13 174 323.9, June 28, 2013.

[7] E. Ravaioli, V. I. Datskov, C. Giloux, G. Kirby, H. H. J. ten Kate, and A. P. Verweij, "New, Coupling Loss Induced, Quench protection system for superconducting accelerator magnets," *IEEE Transactions on Applied Superconductivity*, vol. 24, no. 3, pp. 1–5, June 2014.

[8] E. Ravaioli, B. Auchmann, M. Maciejewski, H. ten Kate, and A. Verweij, "Lumped-element dynamic electro-thermal model of a superconducting magnet," *Cryogenics*, pp. –, 2016. [Online]. Available: http://www.sciencedirect.com/science/article/pii/S0011227516300832

[9] E. Ravaioli, B. Auchmann, G. Chlachidze, M. Maciejewski, G. Sabbi, S. E. Stoynev, and A. Verweij, "Modeling of inter-filament coupling currents and their effect on magnet quench protection," *IEEE Transactions on Applied Superconductivity*, vol. 27, no. 4, pp. 1–8, June 2017.

[10] A. P. Verweij, "Electrodynamics of superconducting cables in accelerator magnets," Ph.D. dissertation, Twente U., Twente, 1995, presented on 15 Sep 1995. [Online]. Available: https://cds.cern.ch/record/292595

[11] M. Wilson, *Superconducting Magnets*, ser. Monographs on Cryogenics. Clarendon Press, 1983.

[12] E. Ravaioli, H. Bajas, V. I. Datskov, V. Desbiolles, J. Feuvrier, G. Kirby, M. Maciejewski, G. Sabbi, H. H. J. ten Kate, and A. P. Verweij, "Protecting a full-scale Nb_3Sn magnet with CLIQ, the new Coupling-Loss-Induced Quench system," *IEEE Transactions on Applied Superconductivity*, vol. 25, no. 3, pp. 1–5, June 2015.

[13] E. Ravaioli, H. Bajas, V. I. Datskov, V. Desbiolles, J. Feuvrier, G. Kirby, M. Maciejewski, H. H. J. ten Kate, A. P. Verweij, and G. Willering, "First implementation of the CLIQ quench protection system on a full-scale accelerator quadrupole magnet," *IEEE Transactions on Applied Superconductivity*, vol. 26, no. 3, pp. 1–5, April 2016.

[14] E. Ravaioli, V. I. Datskov, G. Dib, A. M. Fernandez Navarro, G. Kirby, M. Maciejewski, H. H. J. ten Kate, A. P. Verweij, and G. Willering, "First implementation of the CLIQ quench protection system on a 14-m-long full-scale LHC dipole magnet," *IEEE Transactions on Applied Superconductivity*, vol. 26, no. 4, pp. 1–5, June 2016.

[15] E. Ravaioli, V. Datskov, A. Dudarev, G. Kirby, K. Sperin, H. ten Kate, and A. Verweij, "First experience with the new Coupling Loss Induced Quench system," *Cryogenics*, vol. 60, pp. 33–43, 2014. [Online]. Available: http://www.sciencedirect.com/science/article/pii/S0011227514000162

[16] E. Ravaioli, V. I. Datskov, V. Desbiolles, J. Feuvrier, G. Kirby, M. Maciejewski, K. A. Sperin, H. H. ten Kate, A. P. Verweij, and G. Willering, "Towards an optimized Coupling-loss Induced Quench protection system (CLIQ) for quadrupole magnets," *Physics Procedia*, vol. 67, pp. 215–220, 2015. [Online]. Available: http://www.sciencedirect.com/science/article/pii/S1875389215004186